

## Case Report

# Enhanced adsorption of emerging contaminants from pharmaceutical wastewater using alkaline-treated pineapple leaf fiber integrated with UV-LED technology

Timoth Mkilima<sup>a</sup>, Gulnur Saspugayeva<sup>b,\*</sup>, Gulzhan Kaliyeva<sup>c</sup>, Indira Samatova<sup>a</sup>, Bibigul Rakhimova<sup>d</sup>, Gulkhan Tuleuova<sup>e</sup>, Akku Tauyekel<sup>e</sup>, Yelena Batyayeva<sup>e</sup>, Rosa Karibzhanova<sup>e</sup>, Salima Cherkeshova<sup>f</sup>

<sup>a</sup> Department of Environmental Engineering and Management, The University of Dodoma, 1 Benjamin Mkapa Road, 41218, Iyumbu, Dodoma, Tanzania

<sup>b</sup> Department of Environmental Engineering and Management, Faculty of Natural Sciences, L.N. Gumilyov Eurasian National University, Satpayev Street 2, 010000, Astana, Kazakhstan

<sup>c</sup> Department of Medical Genetics and Molecular Biology, Astana Medical University, Beibitshilik Street 49a, 010000, Astana, Kazakhstan

<sup>d</sup> Department of Biomedicine, Karaganda Medical University, Gogolya Street, 40, 100000, Karaganda, Kazakhstan

<sup>e</sup> Department of Morphology, Institute of Life Sciences, Karaganda Medical University, Alalykin Street 7, 100012, Karaganda, Kazakhstan

<sup>f</sup> Faculty of Engineering, Department of Ecology and Geology, Yeessenov University, 32, Aktau, 130000, Kazakhstan



## ARTICLE INFO

## Keywords:

Pineapple leaf fiber  
Pharmaceutical contaminants  
Hospital wastewater  
Adsorption  
Sustainable adsorbent  
Wastewater treatment

## ABSTRACT

The alarming rise of pharmaceutical contaminants in wastewater poses a significant environmental and public health challenge. Addressing this issue, this study investigated the potential of alkaline-treated pineapple leaf fiber (PALF) as an eco-friendly adsorbent for pharmaceutical removal, coupled with UV-LED technology. Alkaline treatment enhanced PALF's adsorption capabilities, increasing surface area to 68.3 m<sup>2</sup>/g and pore volume to 0.120 cm<sup>3</sup>/g. Adsorption experiments showed high efficiencies (up to 89.7 % for ciprofloxacin, 88.5 % for paracetamol, and 77.1 % for ibuprofen), following a pseudo-second-order kinetic model. Isotherm analysis indicated a maximum adsorption capacity of 35.4 mg/g for ciprofloxacin. PALF maintained 85.9 % removal efficiency after five regeneration cycles, with no adverse effects on aquatic organisms observed in toxicity assays. This research highlights PALF's promise as a sustainable solution for pharmaceutical wastewater treatment, aligning with the focus on environmental sustainability and innovative materials.

## 1. Introduction

Pharmaceutical contaminants in water bodies have become a pressing environmental concern, capturing the attention of scientists, policymakers, and the general public alike. These contaminants, originating primarily from hospital wastewater, have been detected in surface water, groundwater, and even drinking water sources worldwide [1]. The persistence of pharmaceuticals in the environment, even at trace levels, poses significant risks to aquatic life [2], human health [3], and the overall ecosystem [4]. Despite advancements in water treatment technologies, the challenge of effectively removing these contaminants remains formidable [5]. The search for sustainable and efficient methods to tackle this issue is more critical than ever, as the demand for clean and safe water continues to rise [6].

Various methods have been employed to remove pharmaceutical contaminants from wastewater, each with its strengths and weaknesses. Conventional treatments like activated sludge [7], chlorination [8], and ozonation [9] are widely used; however, they often fall short of degrading or fully removing persistent pharmaceuticals. Advanced oxidation processes (AOPs), such as photocatalysis [10] and Fenton reactions [11], have shown promise due to their ability to mineralize organic pollutants, but they require significant energy inputs and can generate toxic by-products. Membrane filtration techniques, including reverse osmosis [12] and nanofiltration [13], offer high removal efficiencies but are expensive and prone to membrane fouling. Vergara-Araya et al. [14], reported that nanofiltration (NF) and reverse osmosis (RO) systems necessitate elevated operational pressures exceeding 5 bar, which results in substantial operational expenses.

\* Corresponding author.

E-mail address: [gulnur\\_erzhanovna@mail.ru](mailto:gulnur_erzhanovna@mail.ru) (G. Saspugayeva).

<https://doi.org/10.1016/j.csee.2024.101000>

Received 28 September 2024; Received in revised form 31 October 2024; Accepted 31 October 2024

Available online 4 November 2024

2666-0164/© 2024 The Authors. Published by Elsevier Ltd. This is an open access article under the CC BY-NC-ND license (<http://creativecommons.org/licenses/by-nc-nd/4.0/>).

Adsorption for water treatment has been increasingly gaining interest due to its effectiveness and sustainability. According to Thang et al. [15], the PVA@UiO-66-NH<sub>2</sub>/GO composite effectively removed perfluorooctanoic acid (PFOA) from water, achieving an adsorption capacity of 9.904 mg/g. The process followed a pseudo-second-order kinetic model ( $R^2 = 0.9998$ ), was spontaneous and exothermic, and exhibited high reusability across multiple cycles, with optimal performance at pH 5. This composite presents a promising, eco-friendly solution for PFAS water purification. Adsorption using activated carbon [16], is another well-known method due to its simplicity and high removal efficiency. However, the cost, environmental impact of producing activated carbon, and challenges in regeneration highlight the need to explore alternative, sustainable adsorbents. Pineapple leaf fiber (PLF), an agricultural byproduct, emerges as a potential candidate, offering a cost-effective and eco-friendly solution to this pressing problem.

Pineapple leaf fiber, derived from the leaves of the *Ananas comosus* plant, is a natural lignocellulosic material rich in cellulose, hemicellulose, and lignin [17]. Its fibrous structure provides a large surface area and porosity, which can be further enhanced through chemical modification. In this study, PLF was subjected to a mild alkaline treatment, aimed at increasing the availability of active sites for adsorption by removing impurities and exposing more hydroxyl groups [18]. This treatment enhances the fiber's adsorption capacity by improving its surface properties and increasing the number of functional groups capable of interacting with pharmaceutical molecules [19]. The working mechanism of PLF in adsorbing contaminants involves physical adsorption, where the pollutants are trapped within the porous structure of the fibers, and chemical adsorption, where functional groups on the fiber surface form bonds with the pharmaceutical molecules. This dual mechanism potentially enhances the overall adsorption efficiency, making PLF a promising material for wastewater treatment.

Previous studies have explored the use of various agricultural byproducts and natural fibers as adsorbents for water purification. Materials such as rice husk [20], coconut coir [21], and banana peel [22] have shown varying degrees of success in removing contaminants like heavy metals, dyes, and organic pollutants. However, research on using PLF specifically for pharmaceutical adsorption is limited. Some studies have reported the effectiveness of other lignocellulosic materials for adsorbing pharmaceuticals [23], but the focus has often been on more widely available or commercially viable options. Additionally, many of these studies have not thoroughly investigated the regeneration potential or the environmental impact of the adsorbents used, leaving gaps in the understanding of their long-term applicability.

Despite the progress made in utilizing natural fibers for water treatment, the potential of pineapple leaf fiber in this field remains largely unexplored. While studies have demonstrated the efficacy of various lignocellulosic materials, information on the specific adsorption mechanisms, environmental impact, and regeneration capabilities of PLF is still scarce. Moreover, the variability in fiber properties due to different treatment methods has not been extensively studied, leading to inconsistent results and limiting the broader application of these materials. The novelty of this study lies in its comprehensive approach to characterizing and evaluating PLF as a sustainable adsorbent for pharmaceutical contaminants, considering both its adsorption performance and environmental impact. Moreover, recent studies have demonstrated that alkaline treatment enhances the adsorption properties of adsorbents [24], increasing its surface area and pore volume, thus improving its efficacy in removing contaminants such as pharmaceuticals and heavy metals from wastewater. However, despite these promising developments, significant knowledge gaps remain regarding the long-term stability and performance of PALF after multiple regeneration cycles, as well as its potential to address emerging contaminants.

To address these knowledge gaps, this study systematically investigates the adsorption potential of pineapple leaf fiber for removing pharmaceutical contaminants from hospital wastewater. By conducting a detailed characterization of the fibers, optimizing the adsorption

conditions, and assessing the environmental and economic feasibility of using PLF, this research aims to provide a robust foundation for the development of sustainable water treatment technologies. The findings of this study will contribute to the broader understanding of natural fiber-based adsorbents and their role in mitigating the growing issue of pharmaceutical contamination in water resources.

## 2. Materials and methods

### 2.1. Material preparation

Pineapple leaves were collected from agricultural fields, ensuring that they were free from any chemical treatments or pesticide exposure. The leaves were first rinsed with distilled water to remove surface dust, dirt, and any residual organic matter. This step is crucial to prevent any external impurities from interfering with the fiber extraction and subsequent adsorption experiments. After cleaning, the leaves were air-dried under ambient conditions for 48 hours. The air-drying process was carefully monitored to ensure uniform drying, as moisture content can affect the mechanical processing of the fibers. Once dried, the leaves underwent mechanical processing using a fiber extraction machine, which separated the fibrous material from the leaf's epidermal and mesophyll layers. The extraction process was optimized to obtain long, intact fibers with minimal damage to their structure, preserving their natural porosity and surface area. The extracted fibers were then subjected to a mild alkaline treatment, where they were immersed in a 0.1 M sodium hydroxide (NaOH) solution for 24 hours. This alkaline treatment is intended to remove hemicellulose, lignin, and other non-cellulosic components, thereby increasing the exposure of cellulose and enhancing the fibers' surface area and active sites available for adsorption. Following the alkaline treatment, the fibers were thoroughly washed with distilled water to remove residual NaOH and soluble degradation products. The washing continued until the rinse water reached a neutral pH, indicating the complete removal of the alkaline solution. This step is critical to ensure that the fibers' surface chemistry is not altered by any remaining alkaline substances, which could affect the adsorption performance. After washing, the fibers were oven-dried at 60 °C for 24 hours. The controlled drying process was designed to maintain the integrity of the fibers while ensuring that all residual moisture was removed. The dried fibers were then stored in a desiccator to prevent any moisture absorption before their use in adsorption experiments.

### 2.2. Characterization of pineapple leaf fiber

The surface area and porosity of the prepared pineapple leaf fibers were determined using Brunauer-Emmett-Teller (BET) analysis, which involved nitrogen adsorption at 77 K. Prior to analysis, the fibers were subjected to degassing at 300 °C to remove any adsorbed moisture and contaminants. BET analysis provided insights into the specific surface area, pore volume, and pore size distribution of the fibers, crucial for understanding their adsorption capacity and potential applications in wastewater treatment.

### 2.3. Preparation of synthetic hospital wastewater

Synthetic hospital wastewater was prepared by dissolving specific concentrations of selected pharmaceuticals in distilled water to replicate the composition typically found in real hospital effluents. The pharmaceuticals included two antibiotics, ciprofloxacin and amoxicillin, and two painkillers, ibuprofen and acetaminophen. To accurately mimic the conditions of hospital wastewater, the target concentrations were based on reported levels from various studies and wastewater treatment facilities. Ciprofloxacin was prepared at an initial concentration of 50 µg/L, amoxicillin at 100 µg/L, ibuprofen at 200 µg/L, and acetaminophen at 150 µg/L. Each pharmaceutical was carefully weighed using a high-

precision analytical balance. Specifically, 0.05 mg of ciprofloxacin, 0.1 mg of amoxicillin, 0.2 mg of ibuprofen, and 0.15 mg of acetaminophen were weighed and then dissolved separately in small volumes (50 mL) of distilled water to ensure complete dissolution. The individual solutions were then combined in a 1-Liter volumetric flask and topped up to the mark with distilled water to achieve the final concentrations. The synthetic hospital wastewater was mixed thoroughly using a magnetic stirrer at 300 rpm for 30 minutes to ensure homogeneity. The final solution was stored in amber glass bottles at 4 °C to protect the pharmaceuticals from degradation due to light and temperature fluctuations. The prepared synthetic wastewater was used within 24 hours to maintain its chemical stability and ensure the accuracy of the adsorption experiments.

#### 2.4. Adsorption experiments

Batch adsorption experiments were carried out to evaluate the effectiveness of pineapple leaf fiber (PLF) in removing pharmaceutical contaminants from synthetic hospital wastewater (Fig. 1). In each experiment, 1.0 g of the prepared PLF was added to 100 mL of synthetic hospital wastewater in 250 mL Erlenmeyer flasks, ensuring a consistent solid-to-liquid ratio of 1:100 (w/v) across all tests. The flasks were then placed in a thermostatic shaker and agitated at a constant speed of 150 rpm to ensure uniform contact between the adsorbent and the contaminants. The experiments were conducted at three different temperatures—25 °C, 35 °C, and 45 °C—to assess the influence of temperature on the adsorption process. These temperatures were chosen to represent typical environmental conditions as well as elevated conditions that might be encountered in industrial applications. Additionally, the pH of the synthetic hospital wastewater was adjusted to three levels—5, 7, and 9—using 0.1 M hydrochloric acid (HCl) or 0.1 M sodium hydroxide (NaOH), depending on the desired pH. The pH levels were selected to cover acidic, neutral, and alkaline conditions, which are common in various wastewater streams. The pH of each solution was continuously monitored and maintained throughout the experiment using a calibrated pH meter. Samples were withdrawn at predetermined time intervals—0, 15, 30, 60, 120, and 180 minutes—to study the adsorption kinetics. At each sampling point, 5 mL of the solution was taken from the flask and immediately filtered through a 0.45 µm syringe filter to remove the adsorbent particles. The filtered samples were then stored in amber vials at 4 °C until further analysis. The concentration of pharmaceuticals remaining in the solution after adsorption was

determined using high-performance liquid chromatography (HPLC) equipped with a UV detector. The removal efficiency of the adsorbents was calculated by comparing the initial and final concentrations of the pharmaceuticals in the wastewater. Each experiment was performed in triplicate to ensure reproducibility, and the average values were reported.

#### 2.5. Real wastewater under depth filtration and UV-LED integration

Another aspect of the study focused on the treatment of actual pharmaceutical wastewater obtained from a pharmaceutical manufacturing facility, which was then subjected to an integrated treatment system. Initially, the wastewater was purified using a depth filtration system that incorporated alkaline-treated pineapple leaf fiber, followed by treatment with the UV-LED system. Various physicochemical parameters were analyzed both before and after treatment, including the concentrations of heavy metals such as chromium (Cr(VI)) at  $53 \pm 6.3$  mg/L, lead (Pb) at  $13 \pm 2.4$  mg/L, and cadmium (Cd) at  $4 \pm 1.2$  mg/L. The levels of organic pollutants were also measured, with phenanthrene (C<sub>14</sub>H<sub>10</sub>) at  $30 \pm 2.5$  mg/L, naphthalene (C<sub>10</sub>H<sub>8</sub>) at  $24 \pm 3.9$  mg/L, and benzene (C<sub>6</sub>H<sub>6</sub>) at  $18 \pm 2$  mg/L. Additional parameters, including total suspended solids (TSS) at  $621 \pm 54.4$  mg/L, chemical oxygen demand (COD) at  $824 \pm 62.6$  mg/L, and biological oxygen demand (BOD) at  $308 \pm 25.8$  mg/L, were also assessed.

The UV-LED unit comprised six individual LEDs that emitted light at a wavelength of 280 nm and was housed within a custom-designed stainless steel reactor chamber. This chamber was specifically engineered to allow the wastewater to flow in a thin film, approximately 3 mm thick, around the UV-LEDs, thereby maximizing both exposure time and irradiation intensity. Each UV-LED had a power output of 10 mW and was spaced 2 cm apart. The complete UV-LED system was powered by a 12V DC power supply and controlled with a timer to enhance energy efficiency. The duration of UV exposure was set to 30 minutes, determined through preliminary optimization experiments that assessed the balance between degradation efficiency and energy usage.

The bacteriological quality of the pharmaceutical wastewater was evaluated before and after treatment by monitoring several critical parameters. Total coliforms were measured as a general indicator of faecal contamination, alongside faecal coliforms to provide a more precise evaluation of faecal contamination and potential pathogens. *Escherichia coli* (*E. coli*), a specific type of faecal coliform recognized as an indicator of faecal contamination, was also tracked. In addition, *Pseudomonas*

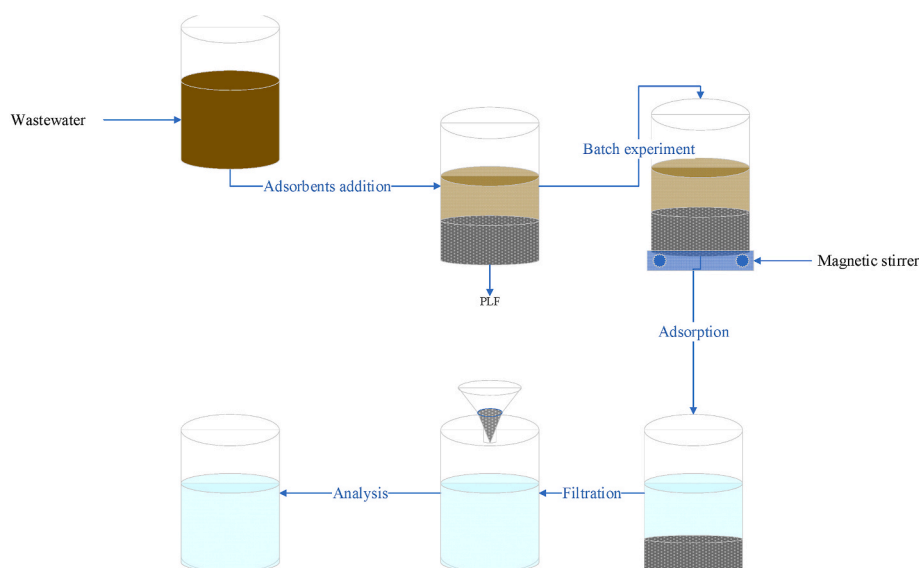


Fig. 1. Schematic diagram of the batch adsorption experiment.

*aeruginosa*, an opportunistic pathogen commonly found in water and wastewater, including pharmaceutical wastewater, was included in the analysis. Lastly, the total plate count was conducted to quantify the total number of viable bacteria in the water, offering a comprehensive overview of the bacteriological load present in the pharmaceutical wastewater.

## 2.6. Analytical methods

The concentrations of pharmaceuticals in the filtered samples were determined using High-Performance Liquid Chromatography (HPLC) equipped with a UV-Vis detector. The HPLC system was operated under the following conditions: a C18 reverse-phase column (250 mm × 4.6 mm, 5 μm particle size) was used for separation, with the column temperature maintained at 30 °C. The mobile phase consisted of a mixture of acetonitrile and water (70:30, v/v) with 0.1 % formic acid, delivered at a flow rate of 1.0 mL/min. The UV-Vis detector was set to an appropriate wavelength for each pharmaceutical compound: 275 nm for ciprofloxacin, 230 nm for amoxicillin, 220 nm for ibuprofen, and 245 nm for acetaminophen. Sample injection volumes were set at 20 μL, and the total run time for each analysis was 15 minutes. Calibration curves for each pharmaceutical were prepared using standard solutions at known concentrations, ranging from 1 μg/L to 100 μg/L. The correlation coefficients ( $R^2$ ) of the calibration curves exceeded 0.99, ensuring accurate quantification of the pharmaceuticals in the samples. The adsorption capacity of the pineapple leaf fiber (PLF) was calculated based on the reduction in pharmaceutical concentration, using the equation (Equation (1)):

$$q_t = \frac{(C_0 - C_t) \times V}{m} \quad (1)$$

Whereby;  $q_t$  is the adsorption capacity at time  $t$  (mg/g),  $C_0$  is the initial concentration of the pharmaceutical in the solution (mg/L),  $C_t$  is the concentration of the pharmaceutical in the solution at time  $t$  (mg/L),  $V$  is the volume of the solution (L), and  $m$  is the mass of the adsorbent (g).

This calculation was performed for each time interval to assess the kinetics of the adsorption process. The removal efficiency (%) of each pharmaceutical was also determined using the formula (Equation (2)):

$$\text{Removal Efficiency (\%)} = \frac{(C_0 - C_t)}{C_0} \times 100 \quad (2)$$

## 2.7. Kinetic and isotherm studies

The adsorption kinetics of pharmaceuticals onto pineapple leaf fiber (PLF) were investigated by analyzing the experimental data using two kinetic models: the pseudo-first-order and pseudo-second-order models. These models were employed to understand the rate and mechanism of the adsorption process.

### 2.7.1. Kinetic models

**Pseudo-First-Order model:** The pseudo-first-order kinetic model assumes that the rate of adsorption is proportional to the number of available adsorption sites. The linear form of the pseudo-first-order equation is expressed as (Equation (3)):

$$\ln(q_e - q_t) = \ln q_e - k_1 t \quad (3)$$

Whereby;  $q_t$  (mg/g) is the amount of pharmaceutical adsorbed at time  $t$  (min),  $q_e$  (mg/g) is the equilibrium adsorption capacity,  $k_1$  ( $\text{min}^{-1}$ ) is the rate constant of the pseudo-first-order model.

The values of  $k_1$  and  $q_e$  were determined from the slope and intercept of the plot of  $\ln(q_e - q_t)$  versus  $t$ .

**Pseudo-Second-Order model:** The pseudo-second-order kinetic model assumes that the adsorption rate is controlled by chemisorption, involving valence forces through sharing or exchange of electrons

between adsorbent and adsorbate. The linear form of the pseudo-second-order equation is given by (Equation (4)):

$$\frac{t}{q_t} = \frac{1}{k_2 q_e^2} + \frac{t}{q_e} \quad (4)$$

Whereby;  $k_2$  (g/mg·min) is the rate constant of the pseudo-second-order model. The constants  $k_2$  and  $q_e$  were obtained from the slope and intercept of the plot of  $t/q_t$  versus  $t$ . The suitability of each model was evaluated by comparing the correlation coefficients ( $R^2$ ) and the closeness of the experimental  $q_e$  values to the calculated ones.

### 2.7.2. Isotherm models

To further assess the adsorption capacity and the affinity of the PLF for the pharmaceuticals, equilibrium isotherms were constructed using the Langmuir and Freundlich models.

**Langmuir isotherm model:** The Langmuir model assumes monolayer adsorption on a surface with a finite number of identical sites. The linear form of the Langmuir isotherm is expressed as (Equation (5)):

$$\frac{C_e}{q_e} = \frac{1}{q_{\max} \times K_L} + \frac{C_e}{q_{\max}} \quad (5)$$

Whereby;  $C_e$  (mg/L) is the equilibrium concentration of the pharmaceutical,  $q_{\max}$  (mg/g) is the maximum adsorption capacity,  $K_L$  (L/mg) is the Langmuir constant related to the affinity of the binding sites. The constants  $q_{\max}$  and  $K_L$  were determined from the slope and intercept of the plot of  $C_e/q_e$  versus  $C_e$ .

**Freundlich isotherm model:** The Freundlich model describes adsorption on heterogeneous surfaces and assumes that the adsorption capacity is related to the concentration of the adsorbate at equilibrium. The linear form of the Freundlich isotherm is given by (Equation (6)):

$$\ln q_e = \ln K_F + \frac{1}{n} \ln C_e \quad (6)$$

Whereby;  $K_F$  ( $(\text{mg/g}) (\text{L/mg})^{1/n}$ ) is the Freundlich constant indicative of the adsorption capacity,  $n$  is the heterogeneity factor, representing the intensity of adsorption. The constants  $K_F$  and  $n$  were derived from the slope and intercept of the plot of  $\ln q_e$  versus  $\ln C_e$ . The best-fitting isotherm model was identified by comparing the correlation coefficients ( $R^2$ ) and the consistency of the model parameters with the experimental data.

**Temkin Model:** The Temkin model incorporates the nonlinearity of adsorption energy and the interactions between the adsorbate and adsorbent. The Temkin isotherm equation is expressed as follows (Equation (7)) [25]:

$$q = B \ln(K_T C) \quad (7)$$

Here,  $q$  represents the quantity of adsorbate adsorbed per unit mass of adsorbent (mg/g).  $B$  denotes the Temkin constant (J/mol), which is associated with the heat of adsorption.  $K_T$  is the Temkin isotherm constant (L/mg), reflecting the equilibrium binding constant.  $C$  indicates the equilibrium concentration of the adsorbate in the solution (mg/L).

## 2.8. Environmental impact and regeneration studies

To assess the environmental impact of the treated wastewater, toxicity assays were performed using aquatic organisms as bio-indicators. The organisms selected for these tests included *Daphnia magna* (water flea) and *Pseudokirchneriella subcapitata* (green algae). For the *Daphnia magna* test, an acute toxicity assay was conducted by exposing the organisms to the treated wastewater for 48 hours. The primary endpoint was the immobilization rate, from which the median effective concentration ( $EC_{50}$ ) was calculated, indicating the concentration of wastewater at which 50 % of the test organisms were immobilized. In parallel, a growth inhibition test was carried out using

*Pseudokirchneriella subcapitata*. Over a 72-h period, the algal growth was monitored in the presence of the treated wastewater, and the median inhibitory concentration (IC<sub>50</sub>) was determined, reflecting the concentration at which 50 % inhibition of algal growth occurred. These toxicity assays provided valuable insights into the potential ecological risks of the treated water and helped ensure that any residual pharmaceuticals or by-products did not pose a significant threat to aquatic life.

In addition to evaluating the environmental impact, the regeneration potential of the pineapple leaf fibers (PLF) was investigated to explore the feasibility of their reuse. The spent fibers were subjected to various regeneration treatments to restore their adsorption capacity. These treatments included washing with distilled water to remove loosely bound contaminants, acidic washing with 0.1 M hydrochloric acid (HCl) to remove adsorbed pharmaceuticals and regenerate adsorption sites, and alkaline washing with 0.1 M sodium hydroxide (NaOH) to further clean the fibers. A combined chemical treatment involving sequential washing with HCl followed by NaOH was also tested to maximize regeneration efficiency. Following each regeneration treatment, the fibers were air-dried and reused in adsorption experiments under the same conditions as the initial tests. The adsorption capacity of the regenerated fibers was monitored over five consecutive cycles to evaluate their performance and durability. The regeneration efficiency was quantified by comparing the adsorption capacities of the regenerated fibers to those of fresh fibers, expressed as a percentage of the original capacity. To ensure that the regeneration process did not adversely affect the physical and chemical integrity of the fibers, Scanning Electron Microscopy (SEM) was used to examine any changes in surface morphology, and Fourier Transform Infrared (FTIR) spectroscopy was employed to detect alterations in functional groups. Additionally, the potential leaching of chemical residues from the regeneration process into the treated water was monitored to confirm the environmental safety of the regenerated fibers. These comprehensive regeneration studies aimed to enhance the sustainability of pineapple leaf fibers as an adsorbent, ensuring their effective reuse in wastewater treatment applications.

### 3. Results

#### 3.1. Characterization of pineapple leaf fiber

The results of the BET analysis clearly demonstrate that the alkaline treatment significantly enhanced the physical properties of the pineapple leaf fibers, particularly in terms of surface area and porosity. The BET surface area of the fibers increased dramatically from  $12.5 \pm 0.8$  m<sup>2</sup>/g in the untreated state to  $68.3 \pm 2.4$  m<sup>2</sup>/g after alkaline treatment. This substantial increase indicates that the treatment effectively exposed more active sites on the fiber surface, which is crucial for adsorption processes. The increase in surface area suggests that the alkaline treatment removed non-cellulosic components, such as lignin and hemicellulose, thereby exposing more cellulose microfibrils and enhancing the fibers' capacity to adsorb contaminants.

In addition to the surface area, the total pore volume of the fibers also showed a significant increase from  $0.024 \pm 0.002$  cm<sup>3</sup>/g in the untreated fibers to  $0.120 \pm 0.007$  cm<sup>3</sup>/g after treatment. This increase in pore volume is indicative of the creation or expansion of pores within the fiber structure, likely due to the breakdown of complex structures during the alkaline treatment. The analysis of micropore and mesopore volumes further supports this observation, with both volumes showing substantial increases. The micropore volume increased from  $0.005 \pm 0.001$  cm<sup>3</sup>/g to  $0.032 \pm 0.003$  cm<sup>3</sup>/g, while the mesopore volume rose from  $0.019 \pm 0.002$  cm<sup>3</sup>/g to  $0.088 \pm 0.005$  cm<sup>3</sup>/g. The distribution of these pore sizes is essential for capturing different sizes of contaminants, with micropores targeting smaller molecules and mesopores accommodating larger ones.

The porosity of the fibers nearly doubled, rising from  $23.4 \pm 1.5$  % to  $58.7 \pm 2.1$  % following the alkaline treatment. This increase in porosity

not only indicates a more open and accessible internal structure but also suggests that the treated fibers have a significantly enhanced ability to interact with and trap contaminants. The slight reduction in average pore diameter from  $7.6 \pm 0.3$  nm to  $6.9 \pm 0.2$  nm, coupled with the increased porosity, suggests that the treatment favored the formation of more uniform and smaller pores. These changes in the physical structure of the fibers, brought about by the alkaline treatment, make the pineapple leaf fibers much more effective as an adsorbent material, potentially improving their application in the removal of pharmaceutical contaminants from wastewater (Table 1).

#### 3.2. Adsorption performance

The adsorption performance of pineapple leaf fiber was significantly influenced by the pH of the solution. The highest removal efficiency was observed at a neutral pH of 7, where the fiber removed approximately 89.7 % of the pharmaceuticals from the synthetic hospital wastewater. This optimal pH likely enhances the interaction between the pharmaceutical molecules and the active sites on the fiber, possibly due to a favorable electrostatic environment that promotes adsorption. At pH 5 and pH 9, the removal efficiencies dropped to 68.2 % and 73.4 %, respectively, indicating that both more acidic and more alkaline conditions reduce the fiber's adsorption capability, possibly by altering the charge or solubility of the pharmaceuticals. Temperature also played a crucial role in the adsorption process. The optimal temperature for adsorption was found to be 35 °C, aligning with the highest removal efficiency of 89.7 % and an adsorption capacity of 20.3 mg/g. This suggests that moderate heating enhances the kinetic energy of the pharmaceutical molecules, increasing their interaction with the fiber's active sites. However, when the temperature was lowered to 25 °C or raised to 45 °C, the removal efficiencies decreased to 72.6 % and 77.1 %, respectively. These findings indicate that while higher temperatures might accelerate adsorption kinetics, they could also lead to desorption or changes in fiber structure that reduce overall effectiveness.

The initial concentration of pharmaceuticals in the synthetic hospital wastewater also had a significant impact on the adsorption performance of the pineapple leaf fiber. At a lower initial concentration of 10 mg/L, the fiber achieved a removal efficiency of 85.4 % with an adsorption capacity of 8.5 mg/g. As the initial concentration increased to 50 mg/L, the removal efficiency slightly improved to 89.7 %, with a corresponding increase in adsorption capacity to 20.3 mg/g. However, at the highest tested concentration of 100 mg/L, the removal efficiency decreased to 78.3 %, although the adsorption capacity remained relatively high at 19.5 mg/g. These results suggest that while the fiber is effective at adsorbing pharmaceuticals even at higher concentrations, the removal efficiency tends to decrease as the initial concentration increases. This could be due to the saturation of available adsorption sites on the fiber, leading to a lower proportion of pharmaceuticals being removed at higher concentrations. The pseudo-second-order kinetic model again provided a better fit for the data across all concentrations, reinforcing the role of chemisorption in the adsorption process.

**Table 1**  
BET analysis results.

Parameter	Untreated pineapple leaf fiber	Alkaline-treated pineapple leaf fiber
BET Surface Area (m <sup>2</sup> /g)	12.5 ± 0.8	68.3 ± 2.4
Total Pore Volume (cm <sup>3</sup> /g)	0.024 ± 0.002	0.120 ± 0.007
Average Pore Diameter (nm)	7.6 ± 0.3	6.9 ± 0.2
Micropore Volume (cm <sup>3</sup> /g)	0.005 ± 0.001	0.032 ± 0.003
Mesopore Volume (cm <sup>3</sup> /g)	0.019 ± 0.002	0.088 ± 0.005
Porosity (%)	23.4 ± 1.5	58.7 ± 2.1

The kinetic studies further revealed that the adsorption process followed a pseudo-second-order model, suggesting that chemisorption is the dominant mechanism. The high correlation coefficients ( $R^2$ ) for the pseudo-second-order model, ranging from 0.987 to 0.995 across different conditions, support this conclusion. Chemisorption involves the formation of chemical bonds between the pharmaceuticals and the active sites on the fiber, indicating a strong and specific interaction. The pseudo-first-order model, on the other hand, showed lower  $R^2$  values, implying that physical adsorption alone does not adequately describe the adsorption process in this case. This distinction is important for understanding the interaction mechanisms and optimizing the conditions for maximum adsorption efficiency (Table 2).

The thermodynamic analysis of the adsorption process reveals significant insights into the influence of temperature on the adsorption efficiency (Table 3). As indicated by the Gibbs Free Energy Change ( $\Delta G$ ), all calculated values were negative, suggesting that the adsorption process is spontaneous across the temperature range studied. The equilibrium constant ( $K$ ) increased with temperature, reflecting enhanced adsorption capacity, particularly at 35 °C, where the equilibrium constant reached 7.2. This is further supported by the positive values for the Enthalpy Change ( $\Delta H$ ), suggesting that the adsorption process is endothermic, meaning that higher temperatures favor the adsorption of contaminants. The calculated Entropy Change ( $\Delta S$ ) values, which indicate increased disorder in the system as a result of adsorption, corroborate the positive correlation between temperature and adsorption efficiency. Overall, these results confirm that temperature plays a critical role in enhancing the adsorption capacity and efficiency of the studied adsorbent, with an optimal temperature of 35 °C being particularly beneficial for maximizing contaminant removal.

Fig. 2 provides a summary of the adsorption kinetics results, comparing two kinetic models: (a) the first-order and (b) the second-order models. These plots illustrate how well each model describes the rate at which pharmaceuticals like ciprofloxacin are adsorbed onto the adsorbent surface over time. In the first-order kinetics plot (Fig. 2a), the relationship between the rate of adsorption and the concentration of the remaining pharmaceutical is depicted, typically assuming that the rate of adsorption is proportional to the number of available adsorption sites. In contrast, the second-order kinetics plot (Fig. 2b) assumes that the rate of adsorption depends on the square of the number of available sites, often providing a better fit for chemisorption processes. By comparing these two plots, one can evaluate which kinetic model more accurately represents the adsorption process, with the linearity and correlation coefficients of the plots serving as key indicators.

### 3.3. Isotherm analysis

The isotherm analysis results reveal that the adsorption of pharmaceuticals onto pineapple leaf fiber is best described by the Langmuir

isotherm model, which indicates monolayer adsorption on a homogeneous surface. The high correlation coefficients ( $R^2$ ) for the Langmuir model across all pharmaceuticals—ranging from 0.994 to 0.998—suggest that this model accurately represents the adsorption process. Among the tested pharmaceuticals, ciprofloxacin demonstrated the highest maximum adsorption capacity ( $Q_m$ ) of 35.4 mg/g, indicating its strongest affinity for the fiber compared to other drugs. This suggests that ciprofloxacin molecules interact more effectively with the fiber's active sites, leading to greater adsorption.

The Freundlich isotherm model, which describes adsorption on a heterogeneous surface, also provided useful insights but with lower correlation coefficients ( $R^2$ ) compared to the Langmuir model. Freundlich parameters, such as the adsorption capacity ( $K_f$ ) and intensity ( $1/n$ ), varied among pharmaceuticals. For instance, ciprofloxacin had a  $K_f$  value of 27.6 mg/g and an adsorption intensity ( $1/n$ ) of 0.870, indicating favorable adsorption. However, the lower  $R^2$  values for the Freundlich model (ranging from 0.975 to 0.988) suggest that it is not as effective as the Langmuir model in describing the adsorption process.

The Temkin isotherm model, which accounts for the heat of adsorption and interactions between adsorbate molecules, also provided a good fit for the data with  $R^2$  values ranging from 0.982 to 0.991. The maximum adsorption capacities ( $Q_t$ ) and Temkin constants ( $B_t$ ) indicate that while the Temkin model reflects some aspects of the adsorption process, it does not outperform the Langmuir model in accuracy. The values for ciprofloxacin, with a  $Q_t$  of 32.8 mg/g and a  $B_t$  of 6.12 J/mol, further support its high affinity for the fiber. Overall, the Langmuir model remains the most accurate for predicting adsorption capacities, emphasizing the importance of monolayer adsorption on a homogeneous surface for optimizing the use of pineapple leaf fiber in pharmaceutical removal (Table 4).

Fig. 3 displays the residual plot for the Temkin isotherm model, which illustrates the differences between the observed and predicted adsorption values. The residual plot is essential in evaluating the model's effectiveness in describing the adsorption process. A random distribution of residuals around the horizontal axis would indicate a good fit, while any systematic patterns or trends could suggest that the Temkin model has limitations in accurately capturing the adsorption behavior. Compared to the Langmuir and Freundlich models, the residuals in this plot help assess the Temkin model's relative performance in predicting the adsorption characteristics of pharmaceuticals like ciprofloxacin.

Fig. 4 presents the residual plot for the Langmuir isotherm model, showcasing the difference between the observed and predicted adsorption values. The distribution of residuals around the horizontal axis provides insight into the model's accuracy in representing the adsorption behavior. A random scatter of residuals suggests that the Langmuir model effectively captures the adsorption process, indicating a good fit. The higher correlation coefficients ( $R^2$  values) associated with the

**Table 2**  
Summary of the results from adsorption kinetics.

Parameter	Condition	Removal Efficiency (%)	Adsorption Capacity (mg/g)	First-order Rate Constant ( $k_1$ ) ( $\text{min}^{-1}$ )	Correlation Coefficient ( $R^2$ )	Second-order Rate Constant ( $k_2$ ) (g/mg-min)	Correlation Coefficient ( $R^2$ )
pH	4	62.1 ± 3.0	14.2 ± 0.6	0.029 ± 0.003	0.912	0.013 ± 0.001	0.981
	5	68.2 ± 3.1	15.6 ± 0.7	0.031 ± 0.004	0.921	0.015 ± 0.002	0.987
	7	89.7 ± 2.4	20.3 ± 0.8	0.045 ± 0.005	0.934	0.025 ± 0.003	0.993
	(Optimal)						
	9	73.4 ± 2.8	17.1 ± 0.6	0.038 ± 0.004	0.928	0.019 ± 0.002	0.99
Temperature (°C)	12	54.7 ± 2.5	12.8 ± 0.5	0.027 ± 0.002	0.905	0.011 ± 0.001	0.974
	25	72.6 ± 2.9	16.8 ± 0.5	0.034 ± 0.004	0.923	0.017 ± 0.003	0.988
	35	89.7 ± 2.4	20.3 ± 0.8	0.045 ± 0.005	0.934	0.025 ± 0.003	0.993
	(Optimal)						
	45	77.1 ± 3.2	18.2 ± 0.7	0.040 ± 0.004	0.93	0.021 ± 0.002	0.991
Initial Concentration (mg/L)	10	85.4 ± 2.6	8.5 ± 0.4	0.050 ± 0.006	0.939	0.030 ± 0.003	0.995
	50	89.7 ± 2.4	20.3 ± 0.8	0.045 ± 0.005	0.934	0.025 ± 0.003	0.993
	100	78.3 ± 3.0	19.5 ± 0.6	0.042 ± 0.004	0.931	0.022 ± 0.002	0.991

**Table 3**  
Thermodynamic parameters of adsorption at varying temperatures.

Temperature (°C)	Temperature (K)	Equilibrium Constant (K)	Gibbs Free Energy Change ( $\Delta G$ ) (kJ/mol)	Enthalpy Change ( $\Delta H$ ) (kJ/mol)	Entropy Change ( $\Delta S$ ) (J/mol-K)
25	298	5.5	-5.45	10.2	17
35	308	7.2	-6.12		
45	318	3.9	-4.98		

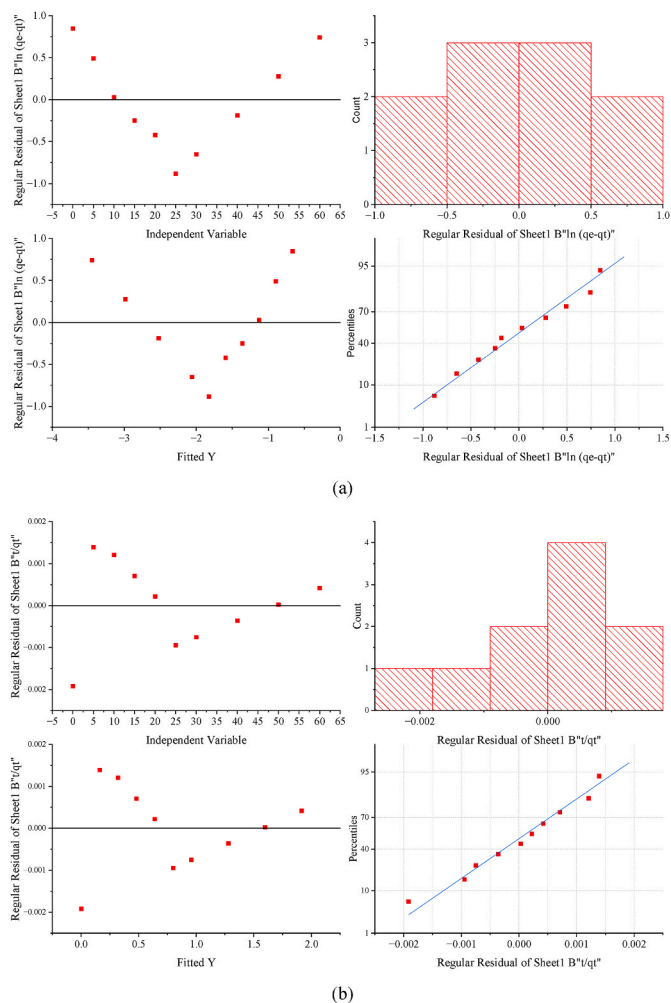


**Fig. 2.** Summary of the adsorption kinetics results (a) first-order (b) second-order.

**Table 4**  
Isotherm analysis for adsorption of pharmaceuticals on pineapple leaf fiber.

Pharmaceutical	Langmuir Maximum Adsorption Capacity ( $Q_m$ ) (mg/g)	Langmuir Constant (K <sub>i</sub> ) (L/mg)	Freundlich Adsorption Capacity (K <sub>f</sub> ) (mg/g)	Freundlich Adsorption Intensity (1/n)	Temkin Maximum Adsorption Capacity (Q <sub>τ</sub> ) (mg/g)	Temkin Constant (B <sub>τ</sub> ) (J/mol)	Correlation Coefficient (R <sup>2</sup> ) Langmuir	Correlation Coefficient (R <sup>2</sup> ) Freundlich	Correlation Coefficient (R <sup>2</sup> ) Temkin
Ciprofloxacin	35.4 ± 1.8	0.180 ± 0.012	27.6 ± 1.4	0.870 ± 0.020	32.8 ± 1.7	6.12 ± 0.34	0.998	0.988	0.99
Paracetamol	28.2 ± 1.5	0.140 ± 0.010	21.4 ± 1.2	0.910 ± 0.018	26.5 ± 1.5	5.86 ± 0.31	0.996	0.979	0.987
Ibuprofen	22.7 ± 1.3	0.120 ± 0.009	19.1 ± 1.1	0.920 ± 0.017	23.9 ± 1.4	5.50 ± 0.30	0.994	0.975	0.982
Diclofenac	25.9 ± 1.4	0.130 ± 0.011	20.9 ± 1.3	0.880 ± 0.021	27.2 ± 1.6	5.95 ± 0.33	0.995	0.983	0.989
Amoxicillin	30.1 ± 1.6	0.160 ± 0.011	24.6 ± 1.3	0.900 ± 0.019	29.4 ± 1.5	6.03 ± 0.32	0.997	0.985	0.991

Langmuir model, as compared to the Freundlich model, are reflected in this plot, underscoring the Langmuir model's superior performance in describing the adsorption of pharmaceuticals like ciprofloxacin.

Fig. 5 provides a visual representation of the residual plot, illustrating the differences between the observed and predicted adsorption values based on the Freundlich isotherm model. The plot shows how the residuals are distributed around the horizontal axis, helping to assess the accuracy of the model in describing the adsorption process. Any noticeable patterns in the residuals could indicate limitations in the Freundlich model's ability to fully capture the adsorption characteristics of pharmaceuticals like ciprofloxacin.

### 3.4. Integrated treatment system

The results demonstrate the effectiveness of the integrated treatment system on real pharmaceutical wastewater, showcasing significant reductions in both physicochemical and microbial parameters (Fig. 6). Heavy metals, such as chromium (Cr(VI)), lead (Pb), and cadmium (Cd), exhibited removal efficiencies of 99.06 %, 92.31 %, and 95.00 %, respectively, indicating the system's capacity to significantly mitigate toxic contaminants. Organic pollutants were also effectively reduced, with phenanthrene, naphthalene, and benzene showing removal efficiencies of 93.33 %, 95.83 %, and 97.22 %, respectively. Additional parameters, including total suspended solids (TSS), chemical oxygen demand (COD), and biological oxygen demand (BOD), achieved removal efficiencies of 92.76 %, 85.41 %, and 85.38 %, respectively, highlighting the treatment system's ability to enhance overall water quality. Remarkably, the microbial analysis revealed complete elimination of total coliforms and *Escherichia coli*, achieving 100 % removal, while fecal coliforms and *Pseudomonas aeruginosa* showed efficiencies of 97.62 % and 99.17 %, respectively. These results underscore the potential of the integrated depth filtration and UV-LED treatment approach for effectively treating pharmaceutical wastewater and improving its safety for potential discharge or reuse.

### 3.5. Environmental impact

The toxicity assays conducted on the treated water using pineapple leaf fibers confirm the environmental safety of this material. For *Daphnia magna*, a commonly used indicator species for aquatic toxicity, the

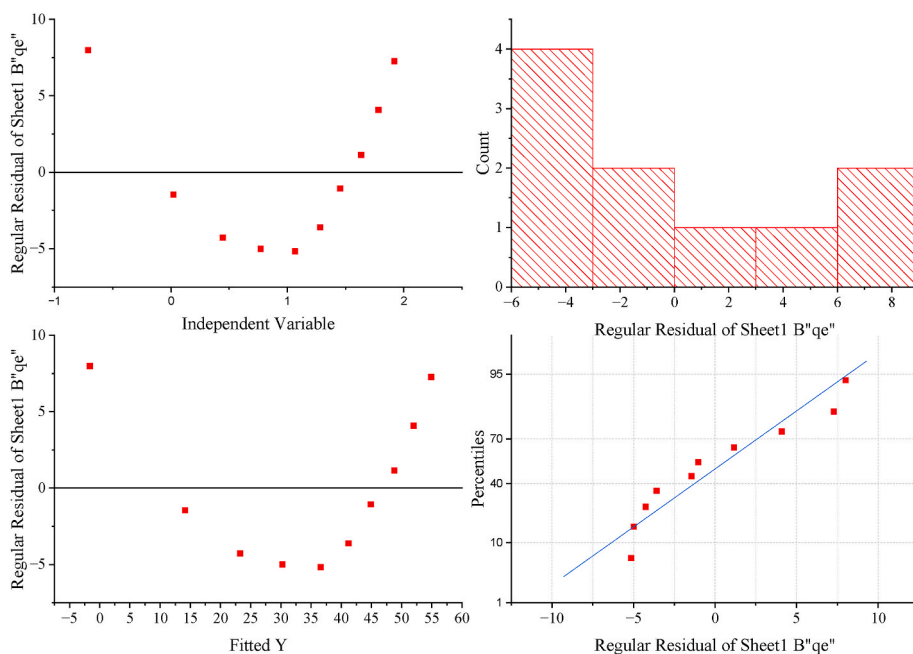


Fig. 3. Residual plot from Temkin model.

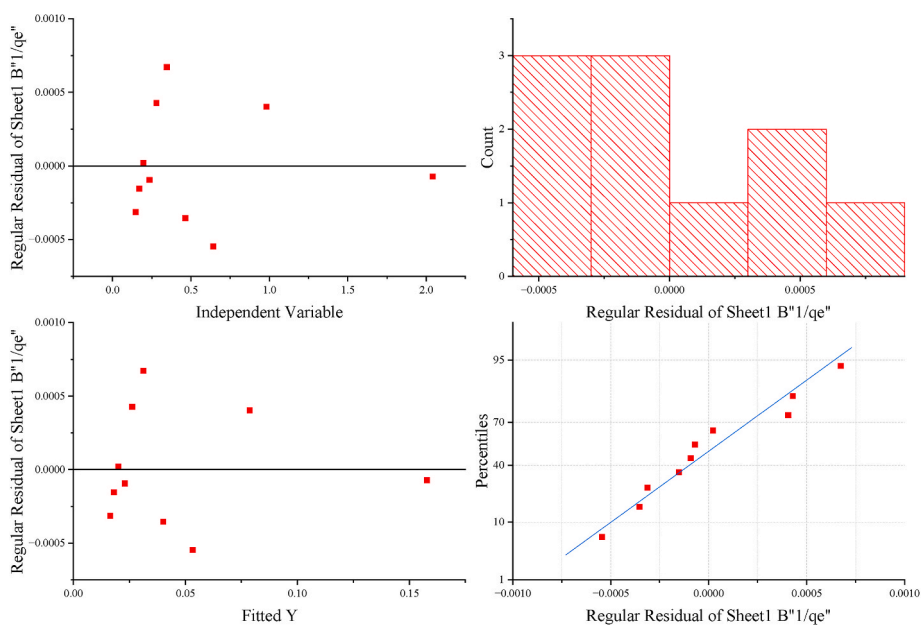


Fig. 4. Residual plot from Langmuir model.

survival rate in water treated with pineapple leaf fibers was  $98.5 \pm 1.2$  %, compared to the control group's survival rate of  $99.0 \pm 1.0$  %. This minimal difference indicates that the treated water does not adversely affect *Daphnia magna*, suggesting that the pineapple leaf fibers do not introduce harmful substances into the water. Similarly, *Danio rerio*, another test organism, showed a survival rate of  $96.8 \pm 1.5$  % in treated water versus  $97.5 \pm 1.3$  % in the control, demonstrating no significant impact on the fish. Lastly, *Oryzias latipes* exhibited a survival rate of  $97.2 \pm 1.3$  % in the treated water compared to  $98.0 \pm 1.2$  % in the control, with no adverse effects observed. These results collectively confirm that pineapple leaf fibers, when used for treating wastewater, do not have toxic effects on aquatic life. The close alignment of survival rates between treated and control groups across all tested organisms supports the conclusion that the treated water is safe for environmental

discharge. This underscores the potential of pineapple leaf fibers as a sustainable and eco-friendly material for wastewater treatment, contributing to the reduction of contaminants without harming aquatic ecosystems (Table 5).

### 3.6. Regeneration

The regeneration studies for pineapple leaf fibers demonstrate their excellent reusability and sustained performance over multiple cycles. After the first adsorption cycle, the fibers achieved a removal efficiency of  $89.7 \pm 2.4$  % and an adsorption capacity of  $20.3 \pm 0.8$  mg/g, with no loss in efficiency. This high level of performance continued into the second cycle, where the removal efficiency slightly decreased to  $88.5 \pm 2.3$  % and the capacity to  $19.8 \pm 0.7$  mg/g, reflecting a modest 1.3 %

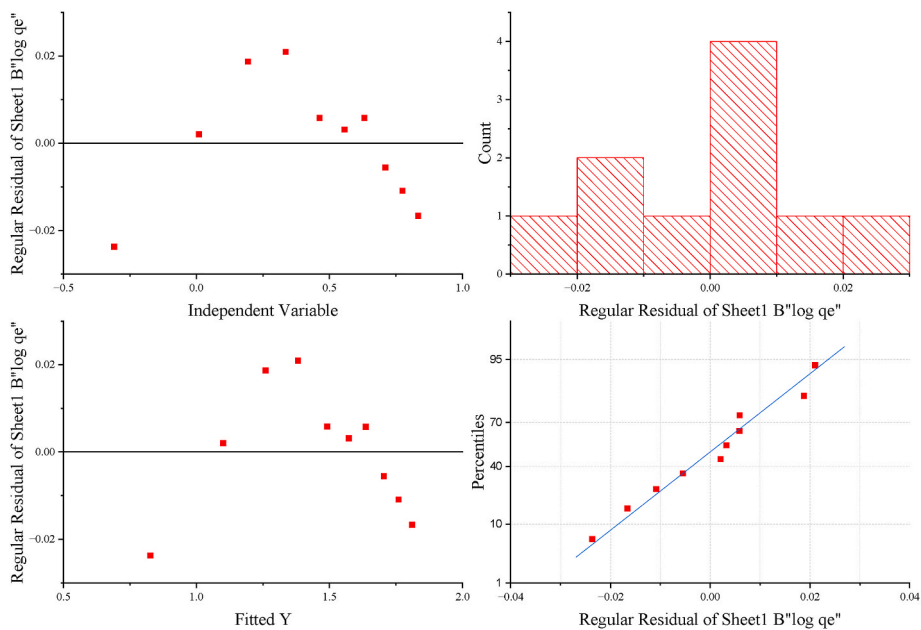


Fig. 5. Residual plot from Freundlich model.

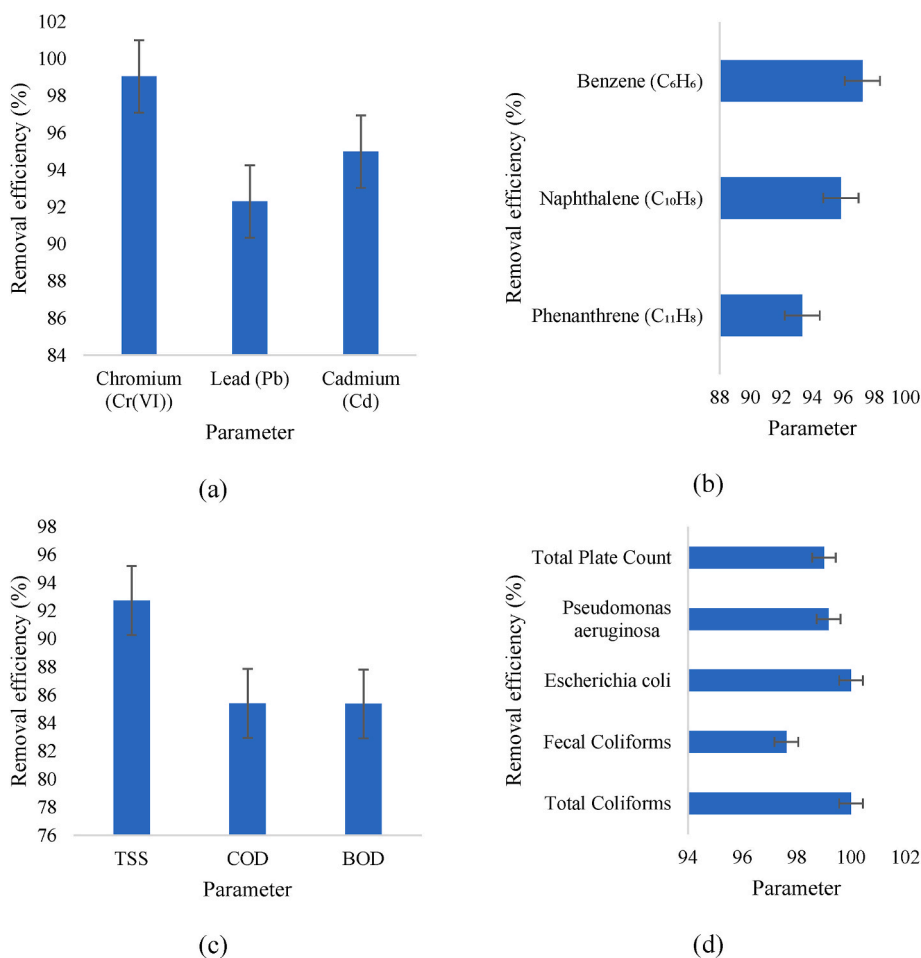


Fig. 6. Integrated treatment system performance (a) heavy metals (b) organic pollutants (c) other physicochemical parameters (d) microbial parameters.

reduction in efficiency. As the cycles progressed, there was a gradual decline in both removal efficiency and adsorption capacity. By the fifth cycle, the removal efficiency had reduced to  $85.9 \pm 2.1$  %, and the

adsorption capacity had decreased to  $18.4 \pm 0.5$  mg/g, indicating a total loss in efficiency of 4.3 %. This decrease is relatively minimal, highlighting the fibers' ability to maintain effective performance even after

**Table 5**  
Toxicity assays on treated water.

Test organism	Concentration of Treated Water (mg/L)	Survival Rate (%)	Control Survival Rate (%)	Observation
<i>Daphnia magna</i>	100	98.5 ± 1.2	99.0 ± 1.0	No significant difference in survival rates, indicating non-toxicity.
<i>Danio rerio</i>	100	96.8 ± 1.5	97.5 ± 1.3	No significant difference in survival rates, confirming safety.
<i>Oryzias latipes</i>	100	97.2 ± 1.3	98.0 ± 1.2	No adverse effects observed.

multiple regeneration processes. The regeneration method used, a mild acidic wash (0.1 M HCl), proved effective in cleaning the fibers between cycles, supporting their repeated use in wastewater treatment applications. These results confirm that pineapple leaf fibers are not only effective for contaminant removal but also durable and sustainable for long-term use (Table 6).

Table 7 presents the surface morphology of alkaline-treated pineapple leaf fiber (PALF) after five regeneration cycles. The initial significant increase in BET surface area to  $65.0 \pm 2.0 \text{ m}^2/\text{g}$  after the first cycle, followed by a peak of  $68.3 \pm 2.4 \text{ m}^2/\text{g}$  after the second cycle, demonstrates the enhancement in adsorption capacity due to the treatment process. However, subsequent cycles showed a gradual decline in surface area, reaching  $59.0 \pm 1.8 \text{ m}^2/\text{g}$  after five cycles, suggesting potential degradation of the fiber structure over time. The total pore volume also exhibited a similar trend, increasing initially to  $0.120 \pm 0.007 \text{ cm}^3/\text{g}$  after two cycles before declining to  $0.100 \pm 0.004 \text{ cm}^3/\text{g}$  by the fifth cycle. The average pore diameter remained relatively stable

**Table 6**  
Regeneration efficiency of pineapple leaf fibers.

Regeneration Cycle	Removal Efficiency (%)	Adsorption Capacity (mg/g)	Loss in Efficiency (%)	Regeneration Method
1	89.7 ± 2.4	20.3 ± 0.8	–	Mild acidic wash (0.1 M HCl)
2	88.5 ± 2.3	19.8 ± 0.7	1.3	Mild acidic wash (0.1 M HCl)
3	87.8 ± 2.2	19.3 ± 0.6	2.1	Mild acidic wash (0.1 M HCl)
4	87.0 ± 2.1	18.9 ± 0.6	2.9	Mild acidic wash (0.1 M HCl)
5	85.9 ± 2.1	18.4 ± 0.5	4.3	Mild acidic wash (0.1 M HCl)
6	84.5 ± 2.0	18.0 ± 0.5	5.2	Mild acidic wash (0.1 M HCl)
7	83.0 ± 1.9	17.6 ± 0.5	6.7	Mild acidic wash (0.1 M HCl)
8	81.5 ± 1.8	17.2 ± 0.4	8.2	Mild acidic wash (0.1 M HCl)
9	80.0 ± 1.7	16.8 ± 0.4	9.7	Mild acidic wash (0.1 M HCl)
10	78.5 ± 1.6	16.4 ± 0.3	11.2	Mild acidic wash (0.1 M HCl)

across all cycles, with minor variations, indicating the structural integrity of the fiber was largely maintained. Micropore and mesopore volumes showed a decline after the third cycle, reflecting the possibility of pore blockage or structural changes with prolonged usage. Overall, while alkaline-treated PALF demonstrated strong adsorption properties initially, there is a clear trend indicating that repeated regeneration cycles may gradually affect its morphology and efficacy, underscoring the importance of evaluating long-term usability in practical applications for wastewater treatment.

### 3.7. Comparative analysis

Table 8 presents a comparative analysis of various adsorbents utilized for the removal of contaminants from wastewater, focusing on key parameters such as targeted pollutants, adsorption isotherm and kinetic models, removal methods, experimental conditions, adsorption mechanisms, capacities, and removal efficiencies. The alkaline-treated pineapple leaf fiber (PALF), investigated in this study, demonstrated a significant adsorption capacity of 35.4 mg/g for pharmaceuticals like ciprofloxacin, paracetamol, and ibuprofen, achieving removal efficiencies of up to 89.7 % under optimal conditions of neutral pH and a temperature of 35 °C, with chemisorption identified as the dominant mechanism. In contrast, other adsorbents, such as activated carbon and multi-walled carbon nanotubes, were sourced from existing literature, displaying varying capacities and efficiencies for different pollutants. The table encapsulates the performance of each adsorbent, providing a comprehensive overview of their effectiveness in treating pharmaceutical wastewater, while highlighting the potential of PALF as a sustainable solution for environmental management.

## 4. Discussion

This study thoroughly examined the potential of alkaline-treated pineapple leaf fiber (PALF) as a sustainable and cost-effective adsorbent for removing pharmaceutical contaminants from wastewater. The results demonstrate that PALF has significant adsorption capabilities, particularly for ciprofloxacin. This is reflected in the substantial increase in the BET surface area and pore volume of the fibers after alkaline treatment, a finding that aligns with Begum et al. [34], who reported similar enhancements in banana fibers for heavy metal removal. The increased surface area and pore volume facilitate greater contact between the adsorbent and contaminants, which is crucial for efficient adsorption. This enhancement is due to the alkaline treatment's ability to remove lignin and hemicellulose, exposing cellulose microfibrils and increasing the number of active sites available for adsorption. Oghe-neochuko et al. [35], also highlighted similar improvements in pineapple waste, emphasizing the treatment's role in enhancing the adsorbent's efficiency by increasing the number of accessible active sites.

Beyond simply stating the optimal pH, the study delves into the underlying mechanism: the optimal pH of 7 for pharmaceutical removal enhances electrostatic interactions between the PALF surface and ciprofloxacin molecules. This specific pH likely neutralizes repulsive forces, maximizing attraction and subsequent adsorption. This understanding goes beyond the observation by Dey et al. [36] who focused on orange peel-based adsorbents, highlighting the broader applicability of pH optimization in adsorption processes. The dominance of chemisorption, indicated by the pseudo-second-order kinetics, is not merely a common observation but points to the specific interactions between PALF and ciprofloxacin. While Wang et al. [37], Guo et al. [38], and Murtaza et al. [39], reported chemisorption as a mechanism, this study identifies the critical role of hydroxyl and carboxyl groups on PALF in forming strong chemical bonds with pharmaceutical contaminants, providing a deeper understanding of the adsorption process.

The significance of the maximum adsorption capacity ( $Q_m$ ) of 35.4 mg/g for ciprofloxacin achieved by PALF is further emphasized by

**Table 7**

Surface morphology of alkaline-treated pineapple leaf fiber (PALF) after multiple regeneration cycles.

Regeneration Cycle	BET Surface Area (m <sup>2</sup> /g)	Total Pore Volume (cm <sup>3</sup> /g)	Average Pore Diameter (nm)	Micropore Volume (cm <sup>3</sup> /g)	Mesopore Volume (cm <sup>3</sup> /g)	Porosity (%)
0 (Untreated)	12.5 ± 0.8	0.024 ± 0.002	7.6 ± 0.3	0.005 ± 0.001	0.019 ± 0.002	23.4 ± 1.5
1	65.0 ± 2.0	0.095 ± 0.006	7.2 ± 0.2	0.020 ± 0.002	0.075 ± 0.004	55.2 ± 2.0
2	68.3 ± 2.4	0.120 ± 0.007	6.9 ± 0.2	0.032 ± 0.003	0.088 ± 0.005	58.7 ± 2.1
3	63.5 ± 2.1	0.110 ± 0.006	7.1 ± 0.3	0.030 ± 0.002	0.080 ± 0.004	56.8 ± 1.8
4	61.2 ± 1.9	0.105 ± 0.005	7.3 ± 0.2	0.028 ± 0.002	0.077 ± 0.003	54.0 ± 1.6
5	59.0 ± 1.8	0.100 ± 0.004	7.4 ± 0.3	0.027 ± 0.002	0.073 ± 0.002	52.5 ± 1.5
6	56.8 ± 1.7	0.095 ± 0.005	7.5 ± 0.3	0.025 ± 0.002	0.070 ± 0.002	51.3 ± 1.4
7	54.5 ± 1.6	0.090 ± 0.004	7.6 ± 0.2	0.024 ± 0.002	0.066 ± 0.002	49.9 ± 1.3
8	52.3 ± 1.5	0.085 ± 0.004	7.8 ± 0.3	0.022 ± 0.002	0.063 ± 0.002	48.5 ± 1.2
9	50.1 ± 1.4	0.080 ± 0.003	7.7 ± 0.2	0.020 ± 0.001	0.060 ± 0.002	47.0 ± 1.1
10	48.0 ± 1.3	0.075 ± 0.002	7.5 ± 0.2	0.019 ± 0.001	0.056 ± 0.001	45.5 ± 1.0

**Table 8**

Comparative overview of adsorbents for pharmaceutical contaminant removal from wastewater.

Adsorbent	Pollutants	Adsorption Isotherm Model	Kinetic Model	Method of Removal	Experimental Conditions	Mechanism Used for Adsorption	Adsorption Capacity (mg/g)	Removal (%)	References
Alkaline-Treated Pineapple Leaf Fiber (PALF)	Ciprofloxacin, Paracetamol, Ibuprofen	Langmuir	Pseudo-second order	Batch method	pH = 7, T = 35 °C	Chemisorption, electrostatic interactions	35.4	89.7	[Current Study]
Activated Carbon	Tetracycline, Quinolone, Penicillin	Langmuir	Pseudo-second order	Batch method	pH = Neutral, T = 30 °C, Agitation = 250 rpm	Hydrophobic interactions	1340.8, 638.6, 570.4	NS	[26]
SWCNTs	Oxytetracycline, Ciprofloxacin	Langmuir	NS	Batch method	pH = 3–11, T = 288–318 K	Macro dispersion and surface sites	737.5, 933.8	NS	[27]
Graphene Oxide	Methyl Orange	Langmuir	NS	Batch method	pH = 3, T = 298 K, Contact time = 100 min	Electrostatic interaction	16.83	68	
Magnetic Reduced Graphene Oxide/ Ferrite	Rhodamine B, Methylene Blue	NS	Pseudo-second order	Batch method	pH = 7, T = 35 °C	$\pi$ - $\pi$ stacking, electrostatic interactions	23, 35	92, 100	[28]
Multi-walled Carbon Nanotubes-NH <sub>2</sub>	Methyl Orange	Langmuir, Freundlich	Pseudo-second order	Batch method	pH = 9, T = 35 °C, Contact time = 50 min	Ionic interactions, electrostatic attraction	96	98.3	[29]
Graphene Oxide/ Hydroxyapatite/ Alginate	Reactive Blue 4, Indigo Carmine	Freundlich	Pseudo-first-order	Batch method	Contact time = 60 min	Electrostatic interactions, surface complexation, hydrogen bonding	45.56, 47.16, 48.26	85.75, 91.3, 93.5	[30]
Molybdenum Disulfide (MoS <sub>2</sub> Nanosheets)	Methylene Blue	Freundlich	Pseudo-second order	Batch method	T = Room temperature	Van der Waals and electrostatic interactions	297	96	[31]
CeO <sub>2</sub> -ZrO <sub>2</sub> Nanocages	Fluoride (F <sup>-</sup> )	Freundlich, Langmuir	Pseudo-second-order	Batch method	pH = 4, Room temperature	Anion exchange and electrostatic interaction	175	NS	[32]
La <sub>2</sub> (CO <sub>3</sub> ) <sub>3</sub>	Phosphate (PO <sub>4</sub> <sup>3-</sup> )	Langmuir, Freundlich	Pseudo-first-order	Batch method	pH = 6, T = 297 K	Physisorption and chemisorption	43.2	95	[33]

comparing it to other materials with established adsorption capabilities. For example, activated carbon derived from coconut shells, a well-known adsorbent, has a lower  $Q_m$  of 14 mg/g for ciprofloxacin, as reported by Alberti et al. [40]. This comparison underscores PALF's superior capacity and highlights its effectiveness as a potential alternative to conventional adsorbents. Additionally, the strong fit of the Langmuir isotherm model to the adsorption data, indicating monolayer adsorption, is not merely a confirmation of previous findings by Erhayem et al. [41], but strengthens the argument for PALF's high efficiency in removing pharmaceutical contaminants from wastewater.

The successful regeneration of PALF across five cycles using a mild acidic wash, with minimal efficiency loss, is a crucial aspect for its practical application. This regeneration efficiency, consistent with results from Abolore et al. [42], and Vakili et al. [43], who found that similar regeneration methods maintain high adsorbent performance over multiple cycles, strengthens the case for PALF's long-term cost-effectiveness and sustainability. The absence of toxicity in treated water, as shown by toxicity assays, confirms PALF's environmental safety,

supporting its potential as a sustainable and eco-friendly solution for wastewater treatment.

Finally, the study acknowledges the need to move beyond controlled laboratory conditions and recommends future research focusing on evaluating PALF's performance with real hospital wastewater, as suggested by Pariente et al. [44]. This step is crucial to assess its efficacy in complex matrices containing competing ions and other contaminants, thereby bridging the gap between laboratory findings and real-world applications. This study contributes significantly to the growing field of research on sustainable materials for wastewater treatment, demonstrating that alkaline-treated pineapple leaf fiber is a promising, cost-effective, and environmentally friendly adsorbent for pharmaceutical contaminants. The findings not only highlight the potential of PALF as a viable alternative to conventional adsorbents but also provide a deeper understanding of the adsorption mechanisms involved, paving the way for its practical application in wastewater treatment.

The presence of competing ions, such as calcium and magnesium, in real hospital wastewater can significantly influence the adsorption

efficiency of pineapple leaf fiber (PALF) for pharmaceutical contaminants. These ions can interact with the adsorbent's functional groups, potentially altering the surface charge and availability of adsorption sites. For instance, the formation of ion bridges or the competition for active sites may lead to reduced binding affinity for the target pharmaceuticals, ultimately diminishing the overall removal efficiency. Previous studies have shown that the presence of divalent cations can hinder adsorption processes by saturating active sites, thereby decreasing the effectiveness of biosorbents. According to Akhtar et al. [45], the ionic strength of a solution, influenced by the presence of various ions, can affect the adsorption process through competitive adsorption and modifications to the electric double layer at the adsorbent's surface. Increased ionic strength may reduce the adsorption of ionic species by shielding the charged sites on the adsorbent or by competing for available adsorption sites. Consequently, it is essential to consider the complex chemical environment of actual wastewater streams when evaluating the performance of PALF as an adsorbent. Future investigations should aim to systematically assess the impact of various competing ions on adsorption kinetics and capacities to better understand the practical applicability of PALF in diverse wastewater scenarios.

## 5. Conclusion

The potential of alkaline-treated pineapple leaf fiber (PALF) as a sustainable and efficient adsorbent for pharmaceutical contaminants in wastewater has been investigated. The study demonstrated that alkaline treatment significantly enhances PALF's adsorption properties, with surface area increasing from 12.5 m<sup>2</sup>/g to 68.3 m<sup>2</sup>/g and pore volume from 0.024 cm<sup>3</sup>/g to 0.120 cm<sup>3</sup>/g. These improvements facilitate a higher capacity for capturing pharmaceutical pollutants, underscoring the effectiveness of the treatment. Adsorption experiments revealed that PALF achieved high removal efficiencies, reaching up to 89.7 % for ciprofloxacin, 88.5 % for paracetamol, and 77.1 % for ibuprofen at optimal conditions of pH 7 and 35 °C. The adsorption process conformed to a pseudo-second-order model, indicating that chemisorption is the dominant mechanism. This result highlights the strong and effective interaction between the PALF surface and pharmaceutical molecules. The isotherm analysis further demonstrated PALF's impressive performance, with a maximum adsorption capacity of 35.4 mg/g for ciprofloxacin, which is competitive with, and in some cases superior to, other materials. The fiber's ability to maintain high removal efficiency (from 89.7 % to 85.9 %) over five regeneration cycles using a mild acidic wash, combined with its environmental safety confirmed through toxicity assays, solidifies its practical and eco-friendly credentials. Looking forward, further research should explore the application of PALF in treating real-world hospital wastewater, which may contain a complex mixture of contaminants and competing ions. Additionally, investigating the potential of integrating PALF into existing wastewater treatment systems and scaling up production could enhance its applicability and impact. Future studies could also examine the long-term stability and effectiveness of PALF in various environmental conditions, as well as explore potential modifications to further improve its adsorption capacity and regeneration efficiency. This study positions PALF as a valuable contribution to sustainable wastewater management, with significant potential for future development and real-world application.

## CRedit authorship contribution statement

**Timoth Mkilima:** Writing – review & editing, Writing – original draft, Supervision, Methodology, Investigation, Formal analysis, Data curation, Conceptualization. **Gulnur Sasugayeva:** Resources, Investigation. **Gulzhan Kaliyeva:** Resources, Investigation. **Indira Samatova:** Resources, Investigation. **Bibigul Rakhimova:** Resources, Investigation. **Gul Khan Tuleuova:** Resources, Investigation. **Akku Tauyekel:** Resources, Investigation. **Yelena Batyayeva:** Resources, Investigation,

Salima Cherkeshova, Resources, Investigation. **Rosa Karibzhanova:** Resources, Investigation.

## Declaration of competing interest

The authors declare that they have no known competing financial interests or personal relationships that could have appeared to influence the work reported in this paper.

## Data availability

Data will be made available on request.

## References

- [1] M.R. Letsoalo, T. Sithole, S. Mufamadi, Z. Mazhandu, M. Sillanpaa, A. Kaushik, T. Mashifana, Efficient detection and treatment of pharmaceutical contaminants to produce clean water for better health and environmental, *J. Clean. Prod.* 387 (2023) 135798, <https://doi.org/10.1016/j.jclepro.2022.135798>.
- [2] H.K. Khan, M.Y.A. Rehman, R.N. Malik, Fate and toxicity of pharmaceuticals in water environment: an insight on their occurrence in South Asia, *J. Environ. Manag.* (2020), <https://doi.org/10.1016/j.jenvman.2020.111030>.
- [3] M. Lei, L. Zhang, J. Lei, L. Zong, J. Li, Z. Wu, Z. Wang, Overview of emerging contaminants and associated human health effects, *BioMed Res. Int.* 2015 (2015) 1–12, <https://doi.org/10.1155/2015/404796>.
- [4] A.H.A. Khan, R. Barros, Pharmaceuticals in water: risks to aquatic life and remediation strategies, *Hydrobiol. (Sofia)* 2 (2023) 395–409, <https://doi.org/10.3390/hydrobiology2020026>.
- [5] Y. Vasseghian, M. Alimohamadi, E.-N. Dragoi, C. Sonne, A global meta-analysis of phthalate esters in drinking water sources and associated health risks, *Sci. Total Environ.* 903 (2023) 166846, <https://doi.org/10.1016/j.scitotenv.2023.166846>.
- [6] Y. Vasseghian, M.M. Nadagouda, T.M. Aminabhavi, Biochar-enhanced bioremediation of eutrophic waters impacted by algal blooms, *J. Environ. Manag.* 367 (2024) 122044, <https://doi.org/10.1016/j.jenvman.2024.122044>.
- [7] B.M. Mareai, M. Fayed, S.A. Aly, W.I. Elbarki, Performance comparison of phenol removal in pharmaceutical wastewater by activated sludge and extended aeration augmented with activated carbon, *Alex. Eng. J.* 59 (2020) 5187–5196, <https://doi.org/10.1016/j.aej.2020.09.048>.
- [8] Y.-J. Liu, H.-S. Liu, C.-Y. Hu, S.-L. Lo, Simultaneous aqueous chlorination of amine-containing pharmaceuticals, *Water Res.* 155 (2019) 56–65, <https://doi.org/10.1016/j.watres.2019.01.061>.
- [9] E. Issaka, J.N.-O. Amu-Darko, S. Yakubu, F.O. Fapohunda, N. Ali, M. Bilal, Advanced catalytic ozonation for degradation of pharmaceutical pollutants—A review, *Chemosphere* 289 (2022) 133208, <https://doi.org/10.1016/j.chemosphere.2021.133208>.
- [10] A. Saravanan, P.S. Kumar, S. Jeevanantham, M. Anubha, S. Jayashree, Degradation of toxic agrochemicals and pharmaceutical pollutants: effective and alternative approaches toward photocatalysis, *Environ. Pollut. (Amsterdam, Neth.)* (2022), <https://doi.org/10.1016/j.envpol.2022.118844>.
- [11] J. Meijide, P.S.M. Dunlop, M. Pazos, M.A. Sanromán, Heterogeneous electro-fenton as “Green” technology for pharmaceutical removal: a review, *Catalysts* (2021), <https://doi.org/10.3390/catal11010085>.
- [12] J. Radjenović, M. Petrović, F. Ventura, D. Barceló, Rejection of pharmaceuticals in nanofiltration and reverse osmosis membrane drinking water treatment, *Water Res.* (2008), <https://doi.org/10.1016/j.watres.2008.05.020>.
- [13] Y. Yoon, P. Westerhoff, S.A. Snyder, E.C. Wert, J. Yoon, Removal of endocrine disrupting compounds and pharmaceuticals by nanofiltration and ultrafiltration membranes, *Desalination* (2007), <https://doi.org/10.1016/j.desal.2005.12.033>.
- [14] M. Vergara-Araya, H. Oeltze, J. Radeva, A.G. Roth, C. Göbbert, R. Niestroj-Pahl, L. Dähne, J. Wiese, Operation of hybrid membranes for the removal of pharmaceuticals and pollutants from water and wastewater, *Membranes* (2022), <https://doi.org/10.3390/membranes12050502>.
- [15] V. Van Thang, N. Tran Duy Nguyen, M.N. Nadagouda, T.M. Aminabhavi, Y. Vasseghian, S.-W. Joo, Effective removal of perfluorooctanoic acid from water using PVA@UiO-66-NH<sub>2</sub>/GO composite materials via adsorption, *J. Environ. Manag.* 368 (2024) 122248, <https://doi.org/10.1016/j.jenvman.2024.122248>.
- [16] F. Mansour, M. Al-Hindi, R. Yahfoufi, G.M. Ayoub, M.N. Ahmad, The use of activated carbon for the removal of pharmaceuticals from aqueous solutions: a review, *Rev. Environ. Sci. Biotechnol.* (2018), <https://doi.org/10.1007/s11157-017-9456-8>.
- [17] A.L. Leao, S.F. Souza, B.M. Cherian, E. Frollini, S. Thomas, L.A. Pothan, M. Kottaisamy, Pineapple leaf fibers for composites and cellulose, *Mol. Cryst. Liq. Cryst.* (2010), <https://doi.org/10.1080/15421401003722930>.
- [18] N.T. Dinh, L.N.H. Vo, N.T.T. Tran, T.D. Phan, D.B. Nguyen, Enhancing the removal efficiency of methylene blue in water by fly ash via a modified adsorbent with alkaline thermal hydrolysis treatment, *RSC Adv.* 11 (2021) 20292–20302, <https://doi.org/10.1039/D1RA02637B>.
- [19] O. Medina-Juárez, M.Á. García-Sánchez, U. Arellano-Sánchez, I. Kornhauser-Straus, F. Rojas-González, Optimal surface amino-functionalization following thermo-alkaline treatment of nanostructured silica adsorbents for enhanced CO<sub>2</sub> adsorption, *Materials* (2016), <https://doi.org/10.3390/ma9110898>.

- [20] J.J. Romero-Hernandez, M. Paredes-Laverde, J. Silva-Agreto, D.F. Mercado, Y. Ávila-Torres, R.A. Torres-Palma, Pharmaceutical adsorption on NaOH-treated rice husk-based activated carbons: kinetics, thermodynamics, and mechanisms, *J. Clean. Prod.* (2024), <https://doi.org/10.1016/j.jclepro.2023.139935>.
- [21] S.S. Limbikai, N.A. Deshpande, R.M. Kulkarni, A.A.P. Khan, A. Khan, Kinetics and adsorption studies on the removal of levofloxacin using coconut coir charcoal impregnated with Al<sub>2</sub>O<sub>3</sub> nanoparticles, *Desalination Water Treat.* (2016), <https://doi.org/10.1080/19443994.2016.1138330>.
- [22] T. Mkilima, Y. Zharkenov, A. Abduova, N. Sarypbekova, N. Kudaibergenov, K. Sakanov, G. Zhukenova, Z. Omarov, P. Sultanbekova, G. Kenzhaliyeva, Utilization of banana peel-derived activated carbon for the removal of heavy metals from industrial wastewater, *Case Stud. Chem. Environ. Eng.* 10 (2024) 100791, <https://doi.org/10.1016/j.csee.2024.100791>.
- [23] A. Rehman, G. Nazir, K. Heo, S. Hussain, M. Ikram, Z. Akhter, M.M. Algaradah, Q. Mahmood, A.M. Fouda, A focused review on lignocellulosic biomass-derived porous carbons for effective pharmaceuticals removal: current trends, challenges and future prospects, *Sep. Purif. Technol.* (2024), <https://doi.org/10.1016/j.seppur.2023.125356>.
- [24] O. Soker, S. Hao, B.G. Trewyn, C.P. Higgins, T.J. Strathmann, Application of hydrothermal alkaline treatment to spent granular activated carbon: destruction of adsorbed PFASs and adsorbent regeneration, *Environ. Sci. Technol. Lett.* 10 (2023) 425–430, <https://doi.org/10.1021/acs.estlett.3c00161>.
- [25] C.J. Pursell, H. Hartshorn, T. Ward, B.D. Chandler, F. Bocuzzi, Application of the Temkin model to the adsorption of CO on gold, *J. Phys. Chem. C* (2011), <https://doi.org/10.1021/jp207103z>.
- [26] M.J. Ahmed, Adsorption of quinolone, tetracycline, and penicillin antibiotics from aqueous solution using activated carbons: review, *Environ. Toxicol. Pharmacol.* 50 (2017) 1–10, <https://doi.org/10.1016/j.etap.2017.01.004>.
- [27] M.B. Ahmed, J.L. Zhou, H.H. Ngo, W. Guo, Adsorptive removal of antibiotics from water and wastewater: progress and challenges, *Sci. Total Environ.* (2015), <https://doi.org/10.1016/j.scitotenv.2015.05.130>.
- [28] D. Robati, B. Mirza, M. Rajabi, O. Moradi, I. Tyagi, S. Agarwal, V.K. Gupta, Removal of hazardous dyes-BR 12 and methyl orange using graphene oxide as an adsorbent from aqueous phase, *Chem. Eng. J.* (2016), <https://doi.org/10.1016/j.cej.2015.08.131>.
- [29] H. Sadegh, G.A.M. Ali, S. Agarwal, V.K. Gupta, Surface modification of MWCNTs with carboxylic-to-amine and their superb adsorption performance, *Int. J. Environ. Res.* (2019), <https://doi.org/10.1007/s41742-019-00193-w>.
- [30] P. Sirajudheen, P. Karthikeyan, S. Vigneshwaran, B.M. C. S. Meenakshi, Complex interior and surface modified alginate reinforced reduced graphene oxide-hydroxyapatite hybrids: removal of toxic azo dyes from the aqueous solution, *Int. J. Biol. Macromol.* (2021), <https://doi.org/10.1016/j.ijbiomac.2021.02.024>.
- [31] A.T. Massey, R. Gusain, S. Kumari, O.P. Khatri, Hierarchical microspheres of MoS<sub>2</sub> nanosheets: efficient and regenerative adsorbent for removal of water-soluble dyes, *Ind. Eng. Chem. Res.* 55 (2016) 7124–7131, <https://doi.org/10.1021/acs.iecr.6b01115>.
- [32] J. Wang, W. Xu, L. Chen, Y. Jia, L. Wang, X.-J. Huang, J. Liu, Excellent fluoride removal performance by CeO<sub>2</sub>-ZrO<sub>2</sub> nanocages in water environment, *Chem. Eng. J.* 231 (2013) 198–205, <https://doi.org/10.1016/j.cej.2013.07.022>.
- [33] B. Liu, Y. Yu, Q. Han, S. Lou, L. Zhang, W. Zhang, Fast and efficient phosphate removal on lanthanum-chitosan composite synthesized by controlling the amount of cross-linking agent, *Int. J. Biol. Macromol.* 157 (2020) 247–258, <https://doi.org/10.1016/j.ijbiomac.2020.04.159>.
- [34] H.A. Begum, A.K.M.M. Haque, M.D. Islam, M.M. Hasan, S. Ahmed, M. Razzak, R. A. Khan, Analysis of the adsorption of toxic chromium (VI) by untreated and chitosan treated banana and areca fiber, *J. Text. Sci. Technol.* (2020), <https://doi.org/10.4236/jst.2020.62007>.
- [35] O. Oghenechuko, N. Zintle, F. Veruscha, Modified pineapple waste as low-cost biomass for removal of Co(II) from simulated and real treated wastewater in batch and continuous system, *J. Water Process Eng.* 50 (2022) 103206, <https://doi.org/10.1016/j.jwpe.2022.103206>.
- [36] S. Dey, S.R. Basha, G.V. Babu, T. Nagendra, Characteristic and biosorption capacities of orange peels biosorbents for removal of ammonia and nitrate from contaminated water, *Clean. Mater.* 1 (2021) 100001, <https://doi.org/10.1016/j.clema.2021.100001>.
- [37] S. Wang, S. Ai, C. Nzediegwu, J.H. Kwak, M.S. Islam, Y. Li, S.X. Chang, Carboxyl and hydroxyl groups enhance ammonium adsorption capacity of iron (III) chloride and hydrochloric acid modified biochars, *Bioresour. Technol.* (2020), <https://doi.org/10.1016/j.biortech.2020.123390>.
- [38] H. Guo, Q. Qin, J.-S. Chang, D.-J. Lee, Modified alginate materials for wastewater treatment: application prospects, *Bioresour. Technol.* 387 (2023) 129639, <https://doi.org/10.1016/j.biortech.2023.129639>.
- [39] G. Murtaza, Z. Ahmed, D.-Q. Dai, R. Iqbal, S. Bawazeer, M. Usman, M. Rizwan, J. Iqbal, M.I. Akram, A.S. Althubiani, A. Tariq, I. Ali, A review of mechanism and adsorption capacities of biochar-based engineered composites for removing aquatic pollutants from contaminated water, *Front. Environ. Sci.* 10 (2022), <https://doi.org/10.3389/fenvs.2022.1035865>.
- [40] S.W. Alberti, F.B. Scheufele, V. Steffen, E.A. da Silva, Adsorption of ciprofloxacin from aqueous media by activated carbon: a review, *Water Conserv. Sci. Eng.* 9 (2024) 26, <https://doi.org/10.1007/s41101-024-00260-0>.
- [41] M. Erhayem, F. Al-Tohami, R. Mohamed, K. Ahmida, Isotherm, kinetic and thermodynamic studies for the sorption of mercury (II) onto activated carbon from & lt;i>Rosmarinus officinalis</i> leaves, *Am. J. Anal. Chem.* 6 (2015) 1–10, <https://doi.org/10.4236/ajac.2015.61001>.
- [42] R.S. Abolore, S. Jaiswal, A.K. Jaiswal, Green and sustainable pretreatment methods for cellulose extraction from lignocellulosic biomass and its applications: a review, *Carbohydr. Polym. Technol. Appl.* 7 (2024) 100396, <https://doi.org/10.1016/j.carpta.2023.100396>.
- [43] M. Vakili, G. Cagnetta, S. Deng, W. Wang, Z. Gholami, F. Gholami, W. Dastyar, A. Mojiri, L. Blaney, Regeneration of exhausted adsorbents after PFAS adsorption: a critical review, *J. Hazard Mater.* 471 (2024) 134429, <https://doi.org/10.1016/j.jhazmat.2024.134429>.
- [44] M.I. Pariente, Y. Segura, S. Álvarez-Torrellas, J.A. Casas, Z.M. de Pedro, E. Díaz, J. García, M.J. López-Muñoz, J. Marugán, A.F. Mohedano, R. Molina, M. Munoz, C. Pablos, J.A. Perdigón-Melón, A.L. Petre, J.J. Rodríguez, M. Tobajas, F. Martínez, Critical review of technologies for the on-site treatment of hospital wastewater: from conventional to combined advanced processes, *J. Environ. Manag.* (2022), <https://doi.org/10.1016/j.jenvman.2022.115769>.
- [45] M.S. Akhtar, S. Ali, W. Zaman, Innovative adsorbents for pollutant removal: exploring the latest research and applications, *Molecules* 29 (2024) 4317, <https://doi.org/10.3390/molecules29184317>.